Heliyon 9 (2023) e22272

Contents lists available at ScienceDirect

Heliyon

journal homepage: www.cell.com/heliyon

Inhibition of SIRT6 aggravates p53-mediated ferroptosis in acute lung injury in mice

Yuanyuan Cao [a,b,1], Tian Peng [b,1], Chenmu Ai [b,1], Zhiwang Li [c], Xiaobao Lei [b], Guicheng Li [b], Tao Li [b], Xiang Wang [b,*], Shumin Cai [a,**]

[a] Department of Critical Care Medicine, Nanfang Hospital, The First School of Clinical Medicine, Southern Medical University, Guangzhou, 510515, PR China
[b] Department of Critical Care Medicine, The First People's Hospital of Chenzhou, The First Affiliated Hospital of Xiangnan University, Xiangnan University, Chenzhou, 423000, PR China
[c] Department of Anesthesiology, The First People's Hospital of Chenzhou, The First Affiliated Hospital of Xiangnan University, Xiangnan University, Chenzhou, 423000, PR China

ARTICLE INFO

Keywords:
Acute lung injury
Ferroptosis
Protein 53
Sirtuin-6
Acetylation

ABSTRACT

Although studies have shown that protein 53 (p53)-mediated ferroptosis is involved in acute lung injury (ALI), the mechanism of its regulation remains unclear. The protective effects of Sirtuin 6 (SIRT6), a histone deacetylase, have been demonstrated in multiple diseases; however, further studies are needed to elucidate the role of SIRT6 in ALI. In the present study, we hypothesize that SIRT6 protects against lipopolysaccharide (LPS)-induced ALI by regulating p53-mediated ferroptosis. We observed that the inhibition of ferroptosis prevented LPS-induced ALI. The knockout of p53 blocked LPS-induced ferroptosis and ALI, suggesting that p53 facilitated ALI by promoting ferroptosis. In addition, the inhibition of SIRT6 aggravated LPS-induced ferroptosis and ALI, while the depression of ferroptosis blocked the exacerbation of lung injury induced by SIRT6 inhibition. The results suggest that SIRT6 protects against ALI by regulating ferroptosis. Furthermore, the inhibition of SIRT6 reinforced the p53 acetylation and the deletion of p53 rescued the exacerbation of ferroptosis induced by SIRT6 inhibition. The findings indicate that SIRT6 regulates the acetylation of p53 and prevents p53-mediated ferroptosis. In conclusion, our results indicate that SIRT6 protects against LPS-induced ALI by regulating p53-mediated ferroptosis, thereby demonstrating that SIRT6 holds great promise as a therapeutic target for ALI.

1. Introduction

Previous studies have reported that ferroptosis, which is a form of regulated cell death characterized by the accumulation of iron-dependent lipid peroxidation, is involved in several diseases, including neurological disorders, cardiovascular, and inflammatory diseases [1,2]. Previous studies have demonstrated the role of ferroptosis in the pathogenesis of acute lung injury (ALI) [3,4]. The

* Corresponding author. Department of Critical Care Medicine, The First People's Hospital of Chenzhou, The first affiliated Hospital of Xiangnan University, Xiangnan University, No.102 Luojiajing, Chenzhou, 423000, Hunan Province, PR China.
** Corresponding author. Department of Critical Care Medicine, Nanfang Hospital, The First School of Clinical Medicine, Southern Medical University, NO. 1838 Guangzhou Avenue North, Guangzhou, 510515, Guangdong Province, PR China.
E-mail addresses: lindy17abc@126.com (X. Wang), 13751845166@163.com (S. Cai).
[1] These authors contributed equally to this work.

https://doi.org/10.1016/j.heliyon.2023.e22272
Received 22 June 2023; Received in revised form 4 November 2023; Accepted 8 November 2023
Available online 11 November 2023

targeting of ferroptosis has been suggested as a potential treatment strategy for ALI; although, further research is needed to fully elucidate the regulatory mechanism of ferroptosis in ALI [5,6].

Ferroptosis is characterized by the accumulation of iron and reactive oxygen species (ROS), which induces the production of lipid hydroperoxides (LOOHs) and cell death [2,7]. Glutathione peroxidase 4 (GPX4) exerts a negative effect on the regulation of ferroptosis by preventing the accumulation of lipid peroxides in a glutathione (GSH)-dependent manner. In addition, the cystine/glutamate transporter system (xc^- system) present in the cell membrane plays a crucial role in GSH production. The function of xc^- system is to transfer cysteine into cells, where it is an important component for GSH production. Several studies suggest that p53 protein plays an important role in the regulation of ferroptosis and is involved in multiple diseases [8,9]. Recent studies have demonstrated that p53 regulates ferroptosis by targeting SLC7A11, a key component of the xc^- system [9,10].

Sirtuin 6 (SIRT6), a member of the sirtuin family of NAD (+)-dependent deacetylases, includes seven members (SIRT1 to SIRT7) [11,12]. SIRT6 has been shown to exert protective effects in various diseases [13,14]; however, the role of SIRT6 in ALI remains unclear. Recent studies have demonstrated that SIRT6 exerts its biological effects by regulating p53-mediated ferroptosis [15,16]. In the present study, we investigate the protective effect of SIRT6 against LPS-induced ALI by the regulation of p53-mediated ferroptosis.

2. Materials and methods

2.1. Chemicals and antibodies

The assay kits for the detection of lipid peroxidation malondialdehyde (MDA) and GSH were purchased from Beyotime Co. (Shanghai, China), while the assay kit for the measurement of GPX4 activity was purchased from Elabscience (Wuhan, China). Fe^{2+} assay kit and antibodies against SLC7A11 and GPX4 were obtained from Abcam (Cambridge, U.K.). The kits for the assay of cytokines (TNF-α, IL-1β, IL-6 and IL-10) and antibodies against β-tubulin and GAPDH were obtained from Abclonal (Wuhan, China). The antibody against acetylated lysine was purchased from PTM Blolabs (Hangzhou, China). OSS-128167, the inhibitor of SIRT6, was purchased from AbMole (Houston, TX, USA). Mouse lung epithelial MLE-12 cells were procured from American Type Culture Collection (ATCC, Manassas, VA, USA).

2.2. Animal model

All experimental procedures involving animals were approved by the Medical Faculty Ethics Committee of Xiangnan University (2022DWLL010, Chenzhou, China). The study was carried out in compliance with the NIH Guidelines for the Care and Use of Laboratory Animals. Adult male C57BL/6 mice (weighing 25–35 g) were procured from the Experimental Animal Centre of South Medical University. The $p53^{-/-}$ mice (C57BL/6 background) were obtained from Xishan Biosciences Inc. (Suzhou, China). Compared with wild type mice kept under similar experimental conditions, the $p53^{-/-}$ mice showed lower weight and was found to lack tumors or other growth and developmental abnormalities which could influence the experimental results. All animals had ad libitum access to food and water and were allowed to acclimatize for one week prior to experimentation.

ALI was induced in mice by an intratracheal instillation of lipopolysaccharides (LPS) as previously described [17]. Briefly, the mice were anesthetized and placed on a warming pad in a supine position. Following midline neck incision in the skin, the trachea was surgically exposed, after which LPS (5 mg/kg body weight) was slowly injected into the trachea of each mouse. The control mice were administered the same volume of normal saline intratracheally. The mice were sacrificed 12 h post LPS/saline administration refers to the results of tendency of ferroptosis and our previous study [18].

2.3. Cell culture and cell viability

Dulbecco's modified Eagle medium (DMEM)- low glucose, supplemented with 10 % fetal bovine serum, penicillin (100 U/mL), and streptomycin (100 units/mL), was used to grow MLE-12 cells at 37 °C in an atmosphere of 5 % CO_2. The *in vitro* LPS-induced ALI model was established by the addition of LPS (5 mg/mL) to the cells for 12 h of stimulation.

After 12 h of LPS stimulation, cell viability was assessed using a 3-[4, 5-dimethylthiazol-2-yl]-2, 5-diphenyltetrazolium bromide (MTT) assay. MTT (0.5 mg/mL) was added to the cells, followed by incubation at 37 °C for 4 h. The absorbance at 570 nm was subsequently determined for each sample using the above-mentioned automatic microplate reader.

2.4. Western blotting

The lung tissue was homogenized, followed by centrifugation at 4 °C. The homogenized tissues were analyzed by Western blot, while the protein concentration of each sample was determined using BCA protein assay. The proteins were separated by 10 % SDS-polyacrylamide gel electrophoresis and were subsequently transferred onto PVDF membranes by electroblotting. The membranes were blocked with 5 % skim milk in PBS at room temperature for 2 h. They were subsequently incubated overnight at 4 °C with primary antibodies against tubulin (1:5000 dilution), SLC7A11 (1:1000 dilution) and GPX4 (1:1000 dilution), followed by incubation with HRP-conjugated secondary antibody (1:5000 dilution). The level of protein expression was visualized using an enhanced chemiluminescence reagent (Absin Biotechnology Co., Ltd., Shanghai, China).

2.5. Determination of GSH content, MDA content and GPX4 activity

The lung tissue and treated cells were homogenized in buffer, followed by centrifugation at 4 °C. and the supernatant was subsequently obtained. The MDA content, GPX4 activity, and the glutathione (GSH)/glutathione disulfide (GSSG) ratio in the lungs and cells were determined using commercial assay kits, according to the manufacturer's instructions.

2.6. Fe^{2+} assays

The Fe^{2+} content was determined using the Fe^{2+} assay kit, according to the manufacturer's instructions. Briefly, the lung tissues were homogenized on ice in Fe^{2+} assay buffer. The samples were subsequently centrifugated, and the supernatant was collected for further assays. The samples were incubated with 5 μL assay buffer for 30 min at 37 °C. The Fe probe (100 μL) was added to each well, followed by incubation at 37 °C in the dark for 1 h. The absorbance at 593 nm was measured using an automatic microplate reader (SpectraMax M5; Molecular Devices, Sunnyvale, CA, USA).

2.7. Histopathological analyses

Twelve hours after LPS treatment, the lung tissue was fixed in 10 % neutral buffered formalin, and embedded in paraffin. After sectioning and staining with hematoxylin and eosin (HE), the pathological changes in the lung tissues were evaluated as previously described [18]. The following parameters were used to quantify the extent of histologic lung injury: i) Neutrophil infiltration; ii) airway epithelial damage; iii) interstitial oedema; iv) hyaline membrane formation; and v) intraalveolar haemorrhage. Each of the parameters had five scores, which corresponded to the following five levels determined by the degree of alteration: Normal = 0; minimal alteration = 1; mild alteration = 2; moderate alteration = 3; and severe alteration = 4. The lung injury score (LIS) was recorded for each criterion.

2.8. Lung wet/dry (W/D) ratio

The lung water content was measured following LPS administration. The right lungs were isolated, blotted, and weighed to obtain the wet weight. Subsequently, the lungs were dried in an incubator at 80 °C for 48 h for dry weight measurement. The lung wet/dry weight ratio, calculated by dividing the wet weight of the lungs by the dry weight, was used for the evaluation of pulmonary oedema in mice.

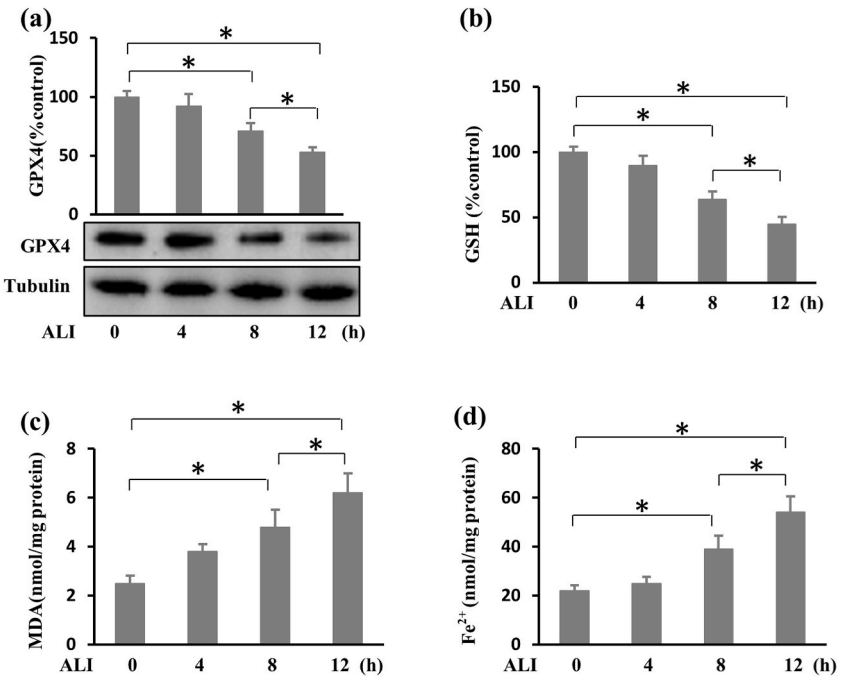

Fig. 1. Ferroptosis is up-regulated in ALI.
Mice were subjected to ALI, and ferroptosis was subsequently determined at several time points. (a) The GPX4 expression was detected by Western blot. The GSH content (b), MDA content (c), and Fe^{2+} level (d) in lungs were detected. Data are presented as mean ± SD (n = 3 or 6 in each group). *P < 0.05 vs. the control groups.

2.9. Determination of pro-inflammatory (TNF-α, IL-1β, IL-6) and anti-inflammatory (IL-10) mediators

The lung tissue was homogenized and centrifuged at 4 °C. The supernatant thus obtained was used for determining the concentrations of TNF-α, IL-1β, IL-6 and IL-10 using a commercial enzyme linked immunosorbent assay kit. The assay results were expressed as μg of cytokine/mg tissue.

2.10. Assessment of p53 acetylation

The p53 acetylation was evaluated by co-immunoprecipitation. The lung tissue was homogenized and centrifuged at 4 °C. The resulting supernatant was incubated overnight with *anti*-p53 antibodies, followed by the addition of protein A/G-coupled agarose beads and further incubation for 2 h. After washing the beads with radioimmunoprecipitation assay (RIPA) buffer, the bead-bound proteins were diluted with 1 × loading buffer and separated by SDS-PAGE. The level of acetylated p53 was subsequently determined by Western blot using a lysine-acetylation antibody.

2.11. Statistical analysis

All data are presented as means ± standard deviation (SD). The differences between groups were analyzed using one-way ANOVA with a LSD multiple-comparison test or a Student's t-test, whichever is appropriate. A p-value <0.05 was considered statistically significant.

3. Results

3.1. Inhibition of ferroptosis alleviates LPS-induced ALI

To investigate the tendency of ferroptosis in ALI, mice were subjected to ALI, followed by the detection of ferroptosis at several time points. The ferroptosis was detected by the expression of GPX4, Fe^{2+} level, and the MDA and GSH content. As shown in Fig. 1, we found that ferroptosis was up-regulated in a time-dependent manner. The ferroptosis, characterized by reduced GPX4 expression (Fig. 1 a) and GSH content (Fig. 1 b) and increased MDA content (Fig. 1 c) and Fe^{2+} level (Fig. 1 d), was found to be significantly activated at 8 h

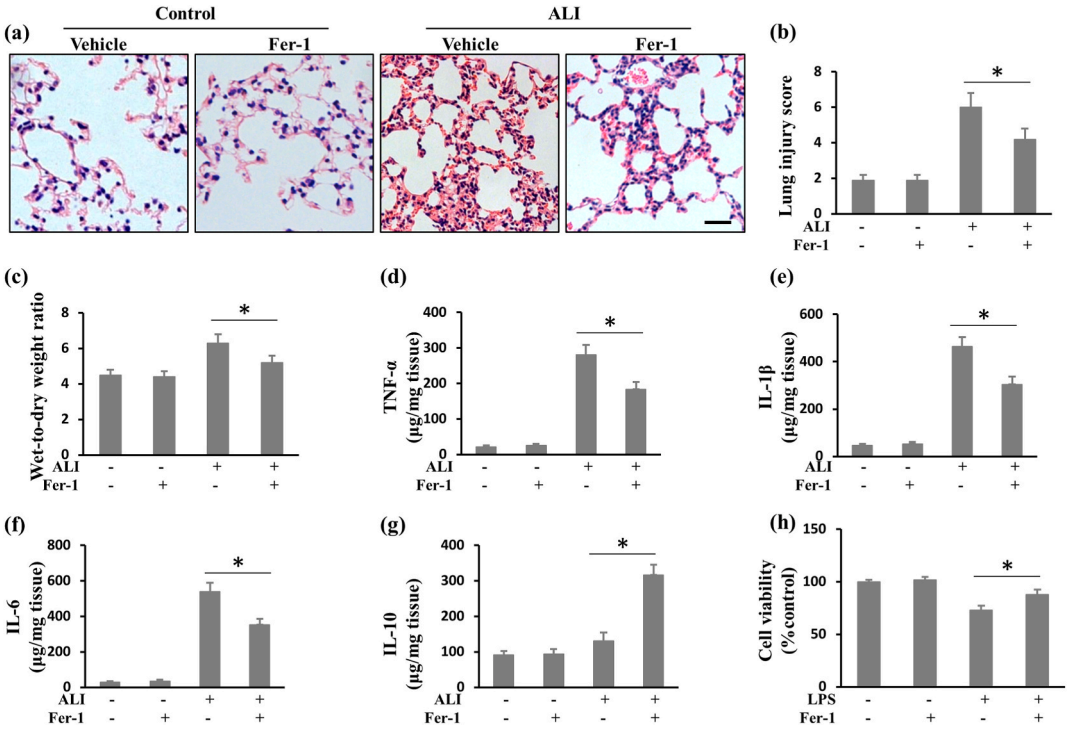

Fig. 2. Inhibition of ferroptosis alleviates LPS-induced ALI
Mice were treated with 0.8 mg/kg of Fer-1 or vehicle and subjected to ALI, and were subsequently sacrificed 12 h after ALI. (a) Histological evaluation was performed after HE-staining (scale bar: 500 μm). (b) Lung injury score. (c) Wet lung/dry lung weight ratio. Levels of TNF-α (d), IL-1β (e), IL-6 (f) and IL-10 (g) in lung tissue. (h) Cells were treated *in vitro* with Fer-1 (2 μM) and exposed to LPS (5 mg/L) for 12 h. Cell viability was detected. Data are presented as mean ± SD (n = 6 in each group). *P < 0.05 vs. the indicated groups.

and 12 h after ALI. Furthermore, the ferroptosis at 12 h post ALI was more serious than that at 8 h post ALI. Thus, 12 h post ALI was selected as the appropriate time point for all subsequent experiments.

In order to elucidate the role of ferroptosis in the pathogenesis of ALI, mice were treated with 0.8 mg/kg of Ferrostatin-1 (Fer-1, a ferroptosis inhibitor) or vehicle and subjected to ALI. They were sacrificed at 12 h post ALI. As shown in Fig. 2 a-c, mice receiving Fer-1 treatment showed improvement in the pathology of injury, along with a decrease in the lung injury score and pulmonary oedema, as evaluated by thelung wet/dry ratio assay, when compared with mice without Fer-1 treatment following ALI. These findings suggest that the ferroptosis inhibitor significantly mitigates the LPS-induced ALI. Futhermore, mice receiving Fer-1 treatment exhibited milder inflammatory response than those without Fer-1 treatment, as reflected by a decrease in the levels of TNF-α, IL-1β and IL-6, and an increase in the levels of IL-10 in lung tissue (Fig. 2 *d*-g). Cells were treated *in vitro* with Fer-1 (2 μM) and exposed to LPS (5 mg/L) for 12 h. We observed that Fer-1 resulted in a significant increase in cell viability after LPS stimulation (Fig. 2 h). These findings showed that the inhibition of ferroptosis alleviated LPS-induced ALI.

3.2. Knockout of p53 prevents LPS-induced ferroptosis and lung injury

In order to study the role of p53 in ferroptosis and the pathogenesis of ALI, wild-type (WT) or p53−/− mice were subjected to ALI, and sacrificed 12 h after LPS instillation. The ferroptosis was evaluated on the basis of the expression levels of GPX4 and SLC7A11, as well as the content of Fe^{2+}, MDA and GSH. As shown in Fig. 3, p53−/− mice showed a significant increase in the GPX4 and SLC7A11 expression (Fig. 3 a-c) and the GSH content (Fig. 3 d), while the Fe^{2+} level (Fig. 3 e) and MDA content (Fig. 3 f) were found to decrease, when compared to WT mice post ALI. This indicates that the deletion of p53 had a significant effect on the prevention of LPS-induced ferroptosis in mice.

Subsequently, the lung injuries were assessed in WT mice and p53−/− mice. As shown in Fig. 4, when compared with WT mice post ALI, p53−/− mice were found to have improved pathological injuries (Fig. 4 a), lower lung injury score (Fig. 4 b), and reduced levels of pulmonary oedema (Fig. 4 c) and pro-inflammatory cytokines (TNF-α, IL-1β and IL-6), while displaying enhanced levels of anti-inflammatory cytokine IL-10 in the lung tissue (Fig. 4 *d*-g). These findings indicate that the deletion of p53 significantly prevented LPS-induced lung injuries, thereby demonstrating the protection offered by deletion of p53 against LPS-induced ALI via the inhibition of ferroptosis.

3.3. Inhibition of SIRT6 exacerbates p53-mediated ferroptosis and lung injury

In order to elucidate the protective effects of SIRT6 in ALI, OSS_128,167 (OSS) was used as the specific inhibitor of SIRT6. Mice treated with OSS (50 mg/kg) or vehicle were subsequently subjected to ALI for 12 h. As shown in Fig. 5 a and b, the p53 acetylation was up-regulated in LPS-treated mice, which was strengthened in the mice receiving OSS treatment following LPS instillation, thereby indicating that SIRT6 induced the deacetylation of p53. Furthermore, the inhibition of SIRT6 exacerbated ferroptosis, as demonstrated

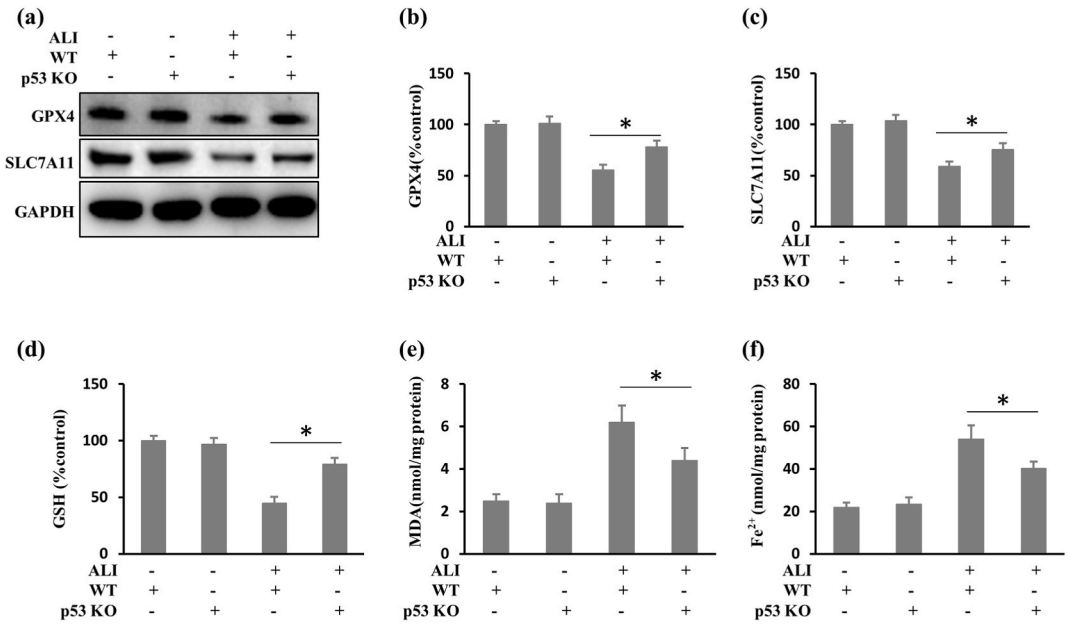

Fig. 3. Knockout of p53 prevents LPS-induced ferroptosis

Wild-type (WT) or p53−/− mice were subjected to ALI and sacrificed post-LPS instillation. (a) The expressions of GPX4 and SLC7A11 were detected by Western blot. Quantification analysis of the GPX4 (b) and SLC7A11 (c) expression levels. The GSH content (d), MDA content, (e) and Fe^{2+} level (f) detected in lung tissue. Data are presented as mean ± SD (n = 3 or 6 in each group). *P < 0.05 vs. the indicated groups.

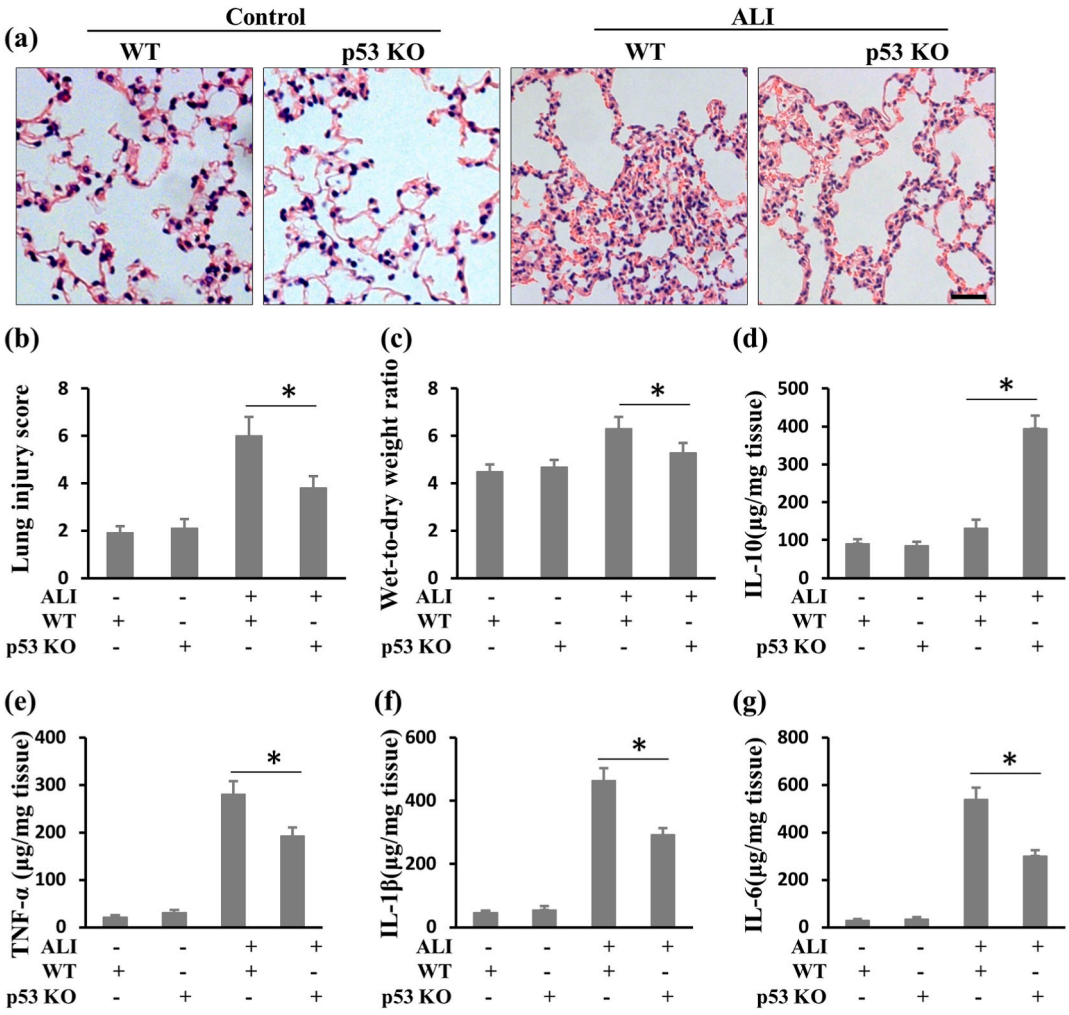

Fig. 4. Knockout of p53 prevents LPS-induced lung injury
Wild-type (WT) or p53−/− mice were subjected to ALI and subsequently sacrificed after 12 h. (a) Histological examination of the tissues was performed after HE-staining (scale bar: 500 μm). (b) Lung injury score. (c) Wet lung/dry lung weight ratio. Levels of IL-10 (d), TNF-α (e), IL-1β (f), and IL-6 (g) in lung tissue. Data are presented as mean ± SD (n = 6 in each group). *P < 0.05 vs. the indicated groups.

by a decrease in the GSH content as well as the expression levels of GPX4 and SLC7A11, and an increase in the Fe^{2+} level and MDA content (Fig. 5 *c*-h). However, the deletion of p53 prominently rescued the aggravation in ferroptosis induced by the SIRT6 inhibition. These results indicate that the inhibition of SIRT6 exacerbates p53-mediated ferroptosis.

To investigate whether SIRT6 protects against ALI by regulating ferroptosis, mice were treated with OSS (50 mg/kg) and thereafter subjected to ALI for 12 h. In this study, the ferroptosis was blocked by p53 deletion or Fer-1 treatment. As shown in Fig. 6, mice treated with OSS showed aggravated pathological injuries (Fig. 6 a), an increase in the lung injury score (Fig. 6 b) and pulmonary oedema (Fig. 6 c), and an up-regulation of pro-inflammatory cytokines (TNF-α, IL-1β and IL-6) in lung tissues (Fig. 6 e-g), when compared to those treated with vehicle post ALI. These findings indicate that the inhibition of SIRT6 significantly exacerbated LPS-induced lung injuries. Interestingly, knockout of p53 or treatment with Fer-1 rescued the aggravation of lung injuries and inflammation induced by SIRT6 inhibition. These findings indicate that SIRT6 offers protection against ALI by regulating the p53-mediated ferroptosis.

4. Discussion

Ferroptosis is a newly identified form of iron-dependent programmed cell death. It differs from other forms of regulated cell death, including apoptosis, pyroptosis and necrosis [19]. Ferroptosis involves the accumulation of iron and reactive oxygen species (ROS), leading to excessive lipid peroxidation in cell membranes and cell death. Under normal conditions, lipid peroxides are reduced by antioxidant systems, including GSH and GPX4. The latter reduces lipid peroxides to alcohols or free hydrogen peroxide in a GSH-dependent manner, which maintains the homeostasis of membrane lipid bilayers. Hence, the accumulation of iron and ROS, GSH depletion and GPX4 inactivation are distinguishing features of ferroptosis. Previous studies have demonstrated the involvement of

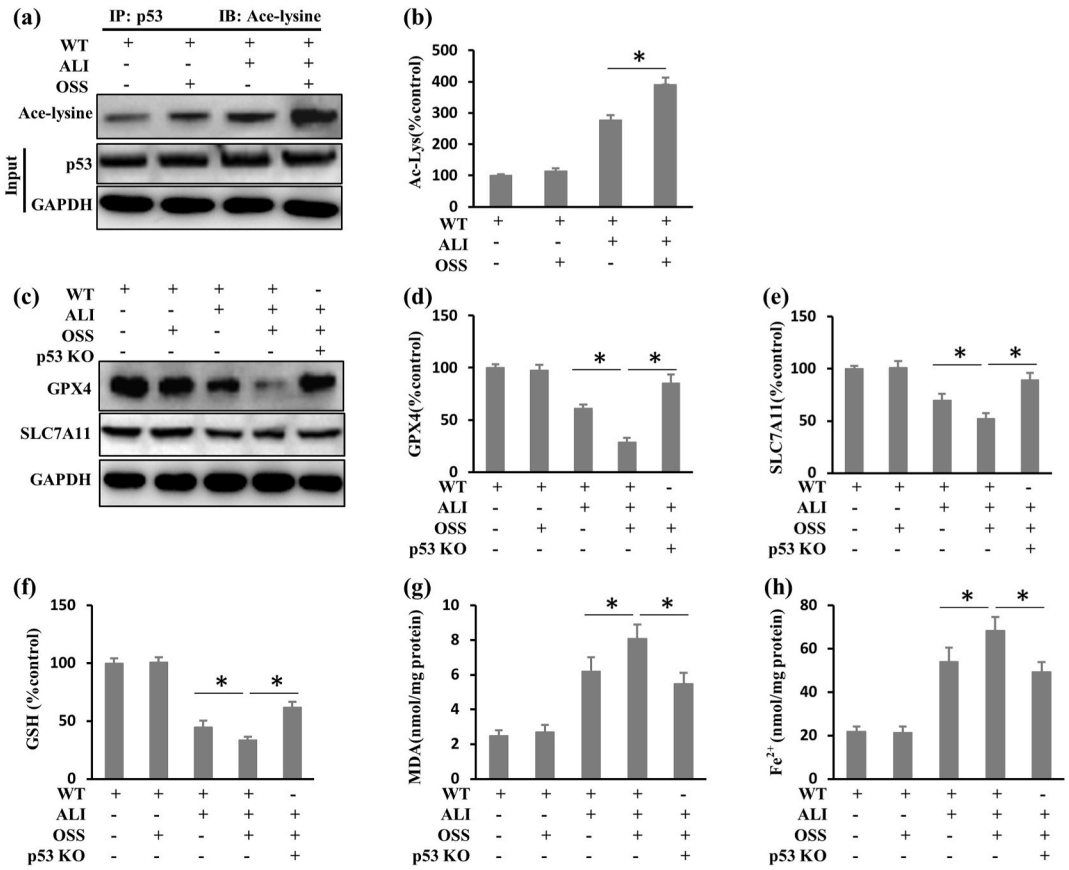

Fig. 5. Inhibition of SIRT6 exacerbates p53-mediated ferroptosis
Mice were subjected to treatment with OSS (50 mg/kg) or vehicle, and thereafter subjected to ALI for 12 h. (a) The p53 acetylation was detected by co-immunoprecipitation. (b) Quantification analysis of the acetylation of p53. (c) Western blot was carried out to detect the expression of GPX4 and SLC7A11. Quantification analysis of the GPX4 (d) and SLC7A11 (e) expression levels. The GSH content (f), The MDA content (g), and the Fe^{2+} level (h) in lung tissue. Data are presented as mean ± SD (n = 3 or 6 in each group). *P < 0.05 vs. the indicated groups.

ferroptosis in ALI [20–22]. The present study showed that the inhibition of ferroptosis significantly mitigated LPS-induced lung injury, which is consistent with the findings of the previous studies.

Several studies suggest that p53 plays a pivotal role in the process of ferroptosis, the mechanism of which includes, but is not limited to, the following pathways: (a) p53 promotes ferroptosis by targeting SLC7A11, an important component of system Xc^-, which functions as a transporter of cystine into cells [23], with the cystine content being involved in GSH synthesis and GPX4 activity, (b) p53 facilitates lipid peroxidation and ferroptosis by promoting SAT1 transcription [24], (c) p53 aggrandizes intracellular iron and accelerates ferroptosis by regulating TFR1 and SLC25a28 [25,26].

A number of studies have reported that p53-mediated ferroptosis plays a key role in several inflammatory diseases [27,28]. In addition, p53-mediated ferroptosis has been shown to play an important role in the ischemia/reperfusion-induced and heat stress-induced ALI [29,30]. The present study demonstrated that the suppression of p53-mediated ferroptosis prevented LPS-induced ALI, thereby suggesting that p53 modulates the pathogenesis of ALI by promoting ferroptosis.

Although previous studies have shown the involvement of SIRT6 in the pathogenesis of multiple diseases, including aging, nervous system diseases, and cardiovascular disorders, the role of SIRT6 in ALI has not yet been fully explored [31,32]. In the present study, we found that the inhibition of SIRT6 exacerbates LPS-induced lung injury, thereby demonstrating the protection offered by SIRT6 in ALI. The role of SIRT6 in regulating ferroptosis has been reported by previous studies [16]. Melatonin has been shown to regulate SIRT6, thereby inhibiting ferroptosis and delaying age-related cataract [33]. SIRT6 has been reported to prevent osteonecrosis of the femoral head by inhibiting ferroptosis [15]. In the present study, the inhibition of SIRT6 was found to enhance LPS-induced ferroptosis in ALI, thereby indicating that ferroptosis is an essential factor involved in the SIRT6-mediated protection against ALI.

Although previous studies have reported the regulating effects of SIRT6 on ferroptosis, the mechanism has not yet been fully explored. In addition, the influence of SIRT6 on p53-mediated ferroptosis needs to be further elucidated. Our study showed that the deletion of p53 rescued the exacerbation of ferroptosis and lung injury induced by SIRT6 inhibition, thereby hinting that SIRT6 protects against ALI by regulating p53-mediated ferroptosis. The posttranslational modification of acetylation is an important regulatory mechanism for the p53. SIRT6 is a NAD (+)-dependent histone deacetylase, and several reports have indicated the importance of

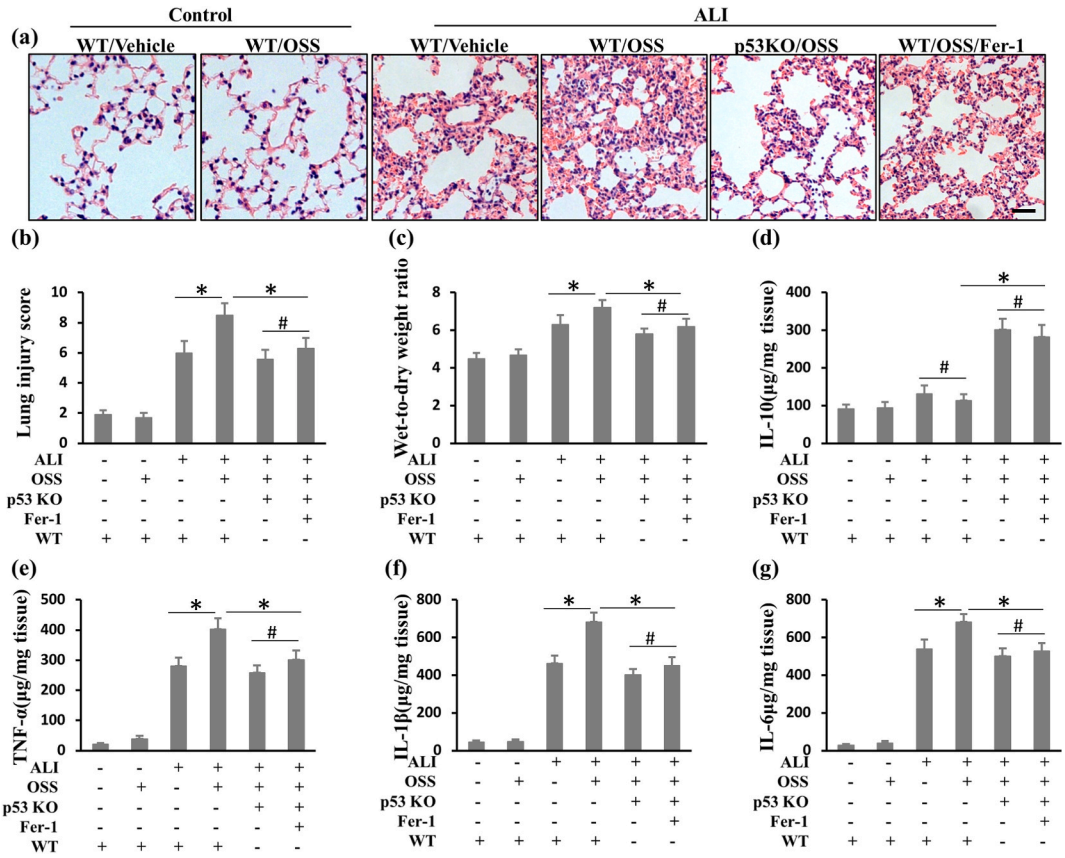

Fig. 6. Blocking ferroptosis and deleting p53 rescues the deterioration of ALI induced by SIRT6 inhibition
Mice were subjected to treatment with OSS (50 mg/kg) or vehicle, and subsequently subjected to ALI for 12 h. The ferroptosis was inhibited by Fer-1 treatment and p53 deletion. (a) Histological evaluation was performed using HE-staining (scale bar: 500 μm). (b) Lung injury score. (c) Wet lung/dry lung weight ratio. Levels of IL-10 (d), TNF-α (e), IL-1β (f), and IL-6 (g) in lung tissue. Data are presented as mean ± SD (n = 6 in each group). *P < 0.05 vs. the indicated groups. #P > 0.05 vs. the indicated groups.

the deacetylation activity of SIRT6 in its biological function [34,35]. In the present study, it was observed that the inhibition of SIRT6 reinforces p53 acetylation, thereby suggesting that SIRT6 prevents ferroptosis by the deacetylation of p53.

Posttranslational acetylation is a key mechanism for the regulation of the cellular distribution and degradation of p53 [36]. It has been shown that the acetylation of p53 influences the cellular distribution of the downstream proteins, including SLC7A11, and ALOX12 [10,37]. In addition, it may also play a role in the regulation of autophagy, with the latter being a key component in the regulation of ferroptosis [38,39]. Furthermore, several lysine sites, including K98, K117, K136, and K382l, have been found in the protein sequence of p53 for acetylation modification, which could have a significant influence on ferroptosis [40]. However, the site for the deacetylation of p53 b y SIRT6 has not yet been elucidated, which warrants further investigation. In conclusion, the results reveal that p53 promotes ferroptosis involved in LPS-induced ALI, and SIRT6 protects against ALI by depressing p53-mediated ferroptosis. Our study indicates that SIRT6 is a potential therapeutic target for ALI; however, the mechanism needs to be explored further in subsequent studies.

Funding information

This work was supported by the Natural Science Foundation of Hunan Province [grant numbers 2023JJ50366, 2022JJ40006, 2023JJ30093]; the Scientific Research Project of Hunan Health Commission [grant number B202317016345]; and the Science and Technology Development Plan Project of Chenzhou [grant numbers ZDYF2020013, ZDYF2020060, ZDYF2020076].

Data availability statement

Data associated with study has not been stored in publicly available repositories. Data will be made available on request.

CRediT authorship contribution statement

Yuanyuan Cao: Writing – original draft, Investigation. **Tian Peng:** Methodology, Investigation. **Chenmu Ai:** Investigation, Funding acquisition, Conceptualization. **Zhiwang Li:** Validation, Software, Resources, Methodology. **Xiaobao Lei:** Formal analysis, Data curation. **Guicheng Li:** Supervision, Resources, Formal analysis, Data curation. **Tao Li:** Validation, Supervision, Project administration, Funding acquisition. **Xiang Wang:** Validation, Software, Methodology, Investigation, Funding acquisition. **Shumin Cai:** Writing – review & editing, Validation, Resources, Funding acquisition.

Declaration of competing interest

The authors have no conflicts of interest to declare.

References

[1] X. Jiang, B.R. Stockwell, M. Conrad, Ferroptosis: mechanisms, biology and role in disease, Nat. Rev. Mol. Cell Biol. 22 (2021) 266–282.
[2] Y. Yu, Y. Yan, F. Niu, Y. Wang, X. Chen, G. Su, Y. Liu, X. Zhao, L. Qian, P. Liu, Y. Xiong, Ferroptosis: a cell death connecting oxidative stress, inflammation and cardiovascular diseases, Cell Death Dis. 7 (2021) 193.
[3] J. Li, K. Lu, F. Sun, S. Tan, X. Zhang, W. Sheng, W. Hao, M. Liu, W. Lv, W. Han, Panaxydol attenuates ferroptosis against LPS-induced acute lung injury in mice by Keap1-Nrf 2/HO-1 pathway, J. Transl. Med. 19 (2021) 96.
[4] P. Liu, Y. Feng, H. Li, X. Chen, G. Wang, S. Xu, Y. Li, L. Zhao, Ferrostatin-1 alleviates lipopolysaccharide-induced acute lung injury via inhibiting ferroptosis, Cell. Mol. Biol. Lett. 25 (2020) 10.
[5] X. Yin, G. Zhu, Q. Wang, Y.D. Fu, J. Wang, B. Xu, Ferroptosis, a new insight into acute lung injury, Front. Pharmacol. 12 (2021), 709538.
[6] J. Zhang, Y. Zheng, Y. Wang, J. Wang, A. Sang, X. Song, X. Li, YAP1 alleviates sepsis-induced acute lung injury via inhibiting ferritinophagy-mediated ferroptosis, Front. Immunol. 13 (2022), 884362.
[7] N. Xing, Q. Du, S. Guo, G. Xiang, Y. Zhang, X. Meng, L. Xiang, S. Wang, Ferroptosis in lung cancer: a novel pathway regulating cell death and a promising target for drug therapy, Cell Death Dis. 9 (2023) 110.
[8] Y. Liu, W. Gu, p53 in ferroptosis regulation: the new weapon for the old guardian, Cell Death Differ. 29 (2022) 895–910.
[9] N. Gao, A.L. Tang, X.Y. Liu, J. Chen, G.Q. Zhang, p53-Dependent ferroptosis pathways in sepsis, Int. Immunopharm. 118 (2023), 110083.
[10] X. Li, W. Xiong, Y. Wang, Y. Li, X. Cheng, W. Liu, p53 activates the lipoxygenase activity of ALOX15B via inhibiting SLC7A11 to induce ferroptosis in bladder cancer cells, Lab. Invest. 103 (2023), 100058.
[11] S. Huang, T. Shao, H. Liu, Q. Wang, T. Li, Q. Zhao, SIRT6 mediates MRTF-A deacetylation in vascular endothelial cells to antagonize oxLDL-induced ICAM-1 transcription, Cell Death Dis. 8 (2022) 96.
[12] C. Bian, H. Zhang, J. Gao, Y. Wang, J. Li, D. Guo, W. Wang, Y. Song, Y. Weng, H. Ren, SIRT6 regulates SREBP1c-induced glucolipid metabolism in liver and pancreas via the AMPKalpha-mTORC1 pathway, Lab. Invest. 102 (2022) 474–484.
[13] Z. Wang, J. Ma, Z. Miao, Y. Sun, M. Dong, Y. Lin, Y. Wu, Z. Sun, Ergothioneine inhibits the progression of osteoarthritis via the Sirt6/NF-kappaB axis both in vitro and in vivo, Int. Immunopharm. 119 (2023), 110211.
[14] F. Yao, X. Lv, Z. Jin, D. Chen, Z. Zheng, J. Yang, L. Ren, B. Wang, W. Wang, J. He, Q. Song, J. Gu, R. Lin, Sirt6 inhibits vascular endothelial cell pyroptosis by regulation of the Lin28b/let-7 pathway in atherosclerosis, Int. Immunopharm. 110 (2022), 109056.
[15] L. Fang, G. Zhang, Y. Wu, Z. Li, S. Gao, L. Zhou, SIRT6 prevents glucocorticoid-induced osteonecrosis of the femoral head in rats, Oxid. Med. Cell. Longev. 2022 (2022), 6360133.
[16] Z. Li, L. Zhou, Y. Du, H. Li, L. Feng, X. Li, X. Han, H. Liu, Polydatin attenuates cisplatin-induced acute kidney injury via SIRT6-mediated autophagy activation, Oxid. Med. Cell. Longev. 2022 (2022), 9035547.
[17] Z. Zhang, X. Wang, C. Ma, Z. Li, H. Chen, Z. Zhang, T. Li, Genipin protects rats against lipopolysaccharide-induced acute lung injury by reinforcing autophagy, Int. Immunopharm. 72 (2019) 21–30.
[18] T. Li, Y. Liu, W. Xu, X. Dai, R. Liu, Y. Gao, Z. Chen, Y. Li, Polydatin mediates Parkin-dependent mitophagy and protects against mitochondria-dependent apoptosis in acute respiratory distress syndrome, Lab. Invest. 99 (2019) 819–829.
[19] X. Chen, J. Li, R. Kang, D.J. Klionsky, D. Tang, Ferroptosis: machinery and regulation, Autophagy 17 (2021) 2054–2081.
[20] Z. Zhongyin, W. Wei, X. Juan, F. Guohua, Isoliquiritin apioside relieves intestinal ischemia/reperfusion-induced acute lung injury by blocking Hif-1 alpha-mediated ferroptosis, Int. Immunopharm. 108 (2022), 108852.
[21] H. Jin, K. Zhao, J. Li, Z. Xu, S. Liao, S. Sun, Matrine alleviates oxidative stress and ferroptosis in severe acute pancreatitis-induced acute lung injury by activating the UCP2/SIRT3/PGC1alpha pathway, Int. Immunopharm. 117 (2023), 109981.
[22] Y. Lv, D. Chen, X. Tian, J. Xiao, C. Xu, L. Du, J. Li, S. Zhou, Y. Chen, R. Zhuang, Y. Gong, B. Ying, F. Gao-Smith, S. Jin, Y. Gao, Protectin conjugates in tissue regeneration 1 alleviates sepsis-induced acute lung injury by inhibiting ferroptosis, J. Transl. Med. 21 (2023) 293.
[23] L. Jiang, N. Kon, T. Li, S.J. Wang, T. Su, H. Hibshoosh, R. Baer, W. Gu, Ferroptosis as a p53-mediated activity during tumour suppression, Nature 520 (2015) 57–62.
[24] Y. Ou, S.J. Wang, D. Li, B. Chu, W. Gu, Activation of SAT1 engages polyamine metabolism with p53-mediated ferroptotic responses, Proc. Natl. Acad. Sci. U. S. A. 113 (2016) E6806–E6812.
[25] L.J. Tang, Y.J. Zhou, X.M. Xiong, N.S. Li, J.J. Zhang, X.J. Luo, J. Peng, Ubiquitin-specific protease 7 promotes ferroptosis via activation of the p53/TfR1 pathway in the rat hearts after ischemia/reperfusion, Free Radic. Biol. Med. 162 (2021) 339–352.
[26] Z. Zhang, M. Guo, M. Shen, D. Kong, F. Zhang, J. Shao, S. Tan, S. Wang, A. Chen, P. Cao, S. Zheng, The BRD7-P53-SLC25A28 axis regulates ferroptosis in hepatic stellate cells, Redox Biol. 36 (2020), 101619.
[27] S. Qin, Y. Ren, B. Feng, X. Wang, J. Liu, J. Zheng, K. Li, M. Chen, T. Chen, H. Mei, X. Fu, ANXA1sp protects against sepsis-induced myocardial injury by inhibiting ferroptosis-induced cardiomyocyte death via SIRT3-mediated p53 deacetylation, Mediat. Inflamm. 2023 (2023), 6638929.
[28] S. Xu, X. Li, Y. Wang, Regulation of the p53-mediated ferroptosis signaling pathway in cerebral ischemia stroke (Review), Exp. Ther. Med. 25 (2023), 113.
[29] Y. Li, Y. Cao, J. Xiao, J. Shang, Q. Tan, F. Ping, W. Huang, F. Wu, H. Zhang, X. Zhang, Inhibitor of apoptosis-stimulating protein of p53 inhibits ferroptosis and alleviates intestinal ischemia/reperfusion-induced acute lung injury, Cell Death Differ. 27 (2020) 2635–2650.
[30] H. Chen, X. Lin, X. Yi, X. Liu, R. Yu, W. Fan, Y. Ling, Y. Liu, W. Xie, SIRT1-mediated p53 deacetylation inhibits ferroptosis and alleviates heat stress-induced lung epithelial cells injury, Int. J. Hyperther. 39 (2022) 977–986.
[31] G. Liu, H. Chen, H. Liu, W. Zhang, J. Zhou, Emerging roles of SIRT6 in human diseases and its modulators, Med. Res. Rev. 41 (2021) 1089–1137.
[32] Z. Guo, P. Li, J. Ge, H. Li, SIRT6 in aging, metabolism, inflammation and cardiovascular diseases, Aging Dis 13 (2022) 1787–1822.
[33] Y. Mi, C. Wei, L. Sun, H. Liu, J. Zhang, J. Luo, X. Yu, J. He, H. Ge, P. Liu, Melatonin inhibits ferroptosis and delays age-related cataract by regulating SIRT6/p-Nrf 2/GPX4 and SIRT6/NCOA4/FTH1 pathways, Biomed. Pharmacother. 157 (2023), 114048.
[34] Z.A. Wang, J.W. Markert, S.D. Whedon, A.M. Yapa, K. Lee, H. Jiang, C. Suarez, H. Lin, L. Farnung, P.A. Cole, Structural basis of sirtuin 6-catalyzed nucleosome deacetylation, J. Am. Chem. Soc. 145 (2023) 6811–6822.

[35] W.H. Liu, J. Zheng, J.L. Feldman, M.A. Klein, V.I. Kuznetsov, C.L. Peterson, P.R. Griffin, J.M. Denu, Multivalent interactions drive nucleosome binding and efficient chromatin deacetylation by SIRT6, Nat. Commun. 11 (2020) 5244.
[36] J.S. Clark, R. Kayed, G. Abate, D. Uberti, P. Kinnon, S. Piccirella, Post-translational modifications of the p53 protein and the impact in alzheimer's disease: a review of the literature, Front. Aging Neurosci. 14 (2022), 835288.
[37] B. Chu, N. Kon, D. Chen, T. Li, T. Liu, L. Jiang, S. Song, O. Tavana, W. Gu, ALOX12 is required for p53-mediated tumour suppression through a distinct ferroptosis pathway, Nat. Cell Biol. 21 (2019) 579–591.
[38] W. Gao, X. Wang, Y. Zhou, X. Wang, Y. Yu, Autophagy, ferroptosis, pyroptosis, and necroptosis in tumor immunotherapy, Signal Transduct. Targeted Ther. 7 (2022) 196.
[39] E. White, Autophagy and p53, Cold Spring Harb Perspect Med 6 (2016), a26120.
[40] S.J. Wang, D. Li, Y. Ou, L. Jiang, Y. Chen, Y. Zhao, W. Gu, Acetylation is crucial for p53-mediated ferroptosis and tumor suppression, Cell Rep. 17 (2016) 366–373.